

Constraints on primordial magnetic fields from the optical depth of the cosmic microwave background

Kerstin E. Kunze,^a Eiichiro Komatsu^{b,c}

^aDepartamento de Física Fundamental and IUFFyM, Universidad de Salamanca, Plaza de la Merced s/n, 37008 Salamanca, Spain

^bMax-Planck-Institut für Astrophysik, Karl-Schwarzschild-Str. 1, 85748 Garching, Germany

^cKavli Institute for the Physics and Mathematics of the Universe (WPI), Todai Institutes for Advanced Study, The University of Tokyo, 5-1-5 Kashiwanoha, Kashiwa, Chiba 277-8583, Japan

E-mail: kkunze@usal.es

Abstract. Damping of magnetic fields via ambipolar diffusion and decay of magnetohydrodynamical (MHD) turbulence in the post decoupling era heats the intergalactic medium (IGM). Delayed recombination of hydrogen atoms in the IGM yields an optical depth to scattering of the cosmic microwave background (CMB). The optical depth generated at $z \gg 10$ does not affect the “reionization bump” of the CMB polarization power spectrum at low multipoles, but affects the temperature and polarization power spectra at high multipoles. Writing the present-day energy density of fields smoothed over the damping scale at the decoupling epoch as $\rho_{B,0} = B_0^2/2$, we constrain B_0 as a function of the spectral index, n_B . Using the Planck 2013 likelihood code that uses the Planck temperature and lensing data together with the WMAP 9-year polarization data, we find the 95% upper bounds of $B_0 < 0.63$, 0.39, and 0.18 nG for $n_B = -2.9$, -2.5 , and -1.5 , respectively. For these spectral indices, the optical depth is dominated by dissipation of the decaying MHD turbulence that occurs shortly after the decoupling epoch. Our limits are stronger than the previous limits ignoring the effects of the fields on ionization history. Inverse Compton scattering of CMB photons off electrons in the heated IGM distorts the thermal spectrum of CMB. Our limits on B_0 imply that the y -type distortion from dissipation of fields in the post decoupling era should be smaller than 10^{-9} , 4×10^{-9} , and 10^{-9} , respectively.

Contents

1	Introduction	1
2	CMB anisotropies with dissipation of magnetic fields in the post-decoupling era	3
3	Parameter estimation	7
4	Conclusions	8
5	Acknowledgements	10

1 Introduction

Damping of magnetic fields affects the thermal and ionization history of the universe. The damping processes before the decoupling epoch can be approximately modeled by damping of three magnetic modes. Of these, damping of the fast magnetosonic waves proceeds in a similar way as the Silk damping of density perturbations, resulting in a damping scale on the order of the Silk scale. Slow magnetosonic and Alfvén waves can avoid damping up to smaller scales, resulting in a larger damping wave number. The value at the decoupling epoch is given by [1, 2]

$$k_{d,dec} = \frac{299.66}{\cos \theta} \left(\frac{B_0}{1 \text{ nG}} \right)^{-1} \text{ Mpc}^{-1}, \quad (1.1)$$

for the best-fit Λ CDM model of the “Planck 2013+WP” data [3]. Here, θ is the angle between the wave vector and the field direction which will be set to zero in this paper.

We assume that the magnetic field is a non-helical and Gaussian random field with its two-point function in Fourier space given by

$$\langle B_i^*(\vec{k}) B_j(\vec{q}) \rangle = (2\pi)^3 \delta(\vec{k} - \vec{q}) P_B(k) \left(\delta_{ij} - \frac{k_i k_j}{k^2} \right), \quad (1.2)$$

where the power spectrum, $P_B(k)$, is assumed to be a power law, $P_B(k) = A_B k^{n_B}$, with the amplitude, A_B , and the spectral index, n_B . This can be expressed in terms of the ensemble average of the present-day magnetic energy density by

$$\langle \rho_{B,0} \rangle = \int \frac{d^3 k}{(2\pi)^3} P_{B,0}(k) e^{-2\left(\frac{k}{k_c}\right)^2}, \quad (1.3)$$

where k_c is a Gaussian smoothing scale. The power-law magnetic power spectrum then gives

$$P_{B,0}(k) = \frac{4\pi^2}{k_c^3} \frac{2^{(n_B+3)/2}}{\Gamma\left(\frac{n_B+3}{2}\right)} \left(\frac{k}{k_c} \right)^{n_B} \langle \rho_{B,0} \rangle. \quad (1.4)$$

For convenience, we define a smoothed magnetic field strength at the present epoch, $B_{\lambda_c,0}$, as $\langle \rho_{B,0} \rangle \equiv \frac{1}{2} B_{\lambda_c,0}^2$, where $\lambda_c \equiv 2\pi/k_c$ is a wavenumber corresponding to k_c . In this

paper, we shall set k_c to the maximal wave number determined by the damping scale at the decoupling epoch, $k_{d,dec}$, given by equation (1.1). For simplicity we shall write $B_0 \equiv B_{\lambda_{d,dec},0}$ throughout the rest of the paper.

Primordial magnetic fields present before the decoupling epoch can generate scalar, vector, and tensor modes of CMB temperature and polarization anisotropies [4–8]. In general, there are two different types; namely, the compensated magnetic mode which is similar to an isocurvature mode, and the passive mode due to the presence of anisotropic stress of the magnetic field before neutrino decoupling. The latter is just like a curvature mode with its amplitude determined by the magnetic anisotropic stress and the time of generation of the primordial magnetic field. These can be important contributions to the CMB anisotropies, depending on the magnetic field parameters. On small angular scales, the scalar compensated mode as well as the vector mode for nG fields with positive spectral indices, $n_B > 0$, can dominate over the primary CMB anisotropies. On large angular scales, the tensor compensated mode for a few nG fields with a nearly scale invariant spectrum, $n_B = -2.9$, can dominate [9]. However, here we shall ignore these contributions and derive constraints focusing only on the effect of dissipation of fields in the post decoupling era. Since we only consider $n_B < 0$, the former contributions can be ignored. The limit we obtain for $n_B = -2.9$ is smaller than nG, making the latter contributions sub-dominant. In any case, including these contributions in the analysis would make the constraints on B_0 stronger.

After the decoupling epoch, magnetic fields are damped by ambipolar diffusion and decaying MHD turbulence [10]. This leads to a change in the ionization and thermal history, hence the visibility function of CMB anisotropies. In ref. [11], we have calculated the thermal and ionization history of the IGM including dissipation of fields. Ionization gives an optical depth to Thomson scattering of the CMB. By writing the total optical depth as $\tau_{tot}(B_0, n_B) = \tau_{tot}(B_0 = 0) + \Delta\tau(B_0, n_B)$, the additional contribution from dissipation of magnetic fields $\Delta\tau$ is given by¹

$$\begin{aligned} \Delta\tau(B_0, n_B) = & 0.0241 \left(\frac{B_0}{\text{nG}} \right)^{1.547} (-n_B)^{-0.0370} \\ & \times e^{-5.2815 \times 10^{-12} (-n_B)^{23.8731} + 5.4 \times 10^{-3} \left(\frac{B_0}{\text{nG}} \right)^{3.3706} - 7.1 \times 10^{-3} (-n_B)^{1.948} \left(\frac{B_0}{\text{nG}} \right)^{2.0713}} \end{aligned} \quad (1.5)$$

for $n_B < 0$.

In general, there are two important contributions to the total optical depth out to the decoupling epoch: the contribution due to reionization, τ_{reio} , and that generated at high redshifts close to decoupling, τ_{high-z} . Hence $\tau_{tot} = \tau_{reio} + \tau_{high-z}$. Whereas τ_{reio} determines the CMB polarization angular power spectrum at low multipoles (“reionization bump”), the total optical depth out to decoupling determines the overall suppression of the temperature power spectrum at high multipoles as $C_\ell^{TT} \rightarrow C_\ell^{TT} e^{-2\tau_{tot}}$. As the contribution to the optical depth from dissipation of fields comes from high redshifts, $z \gg 10$, it has little effect on τ_{reio} and hence the CMB polarization power spectrum at low multipoles. Therefore, the change in the amplitude of the temperature angular power spectrum induced by the magnetic field dissipation is determined by $\Delta\tau(B_0, n_B)$, and the temperature data at high multipoles will be

¹This formula is a minor update of the formula we gave in ref. [11]. We now use the Planck 13+WP best fit cosmological parameters. Following ref. [9, 12], we calculate the photoionization rates at the photon temperature instead of the electron temperature in the modified version of **Recfast++**, and include the collisional ionization. Finally, we have also corrected a numerical error in the amplitude of the ambipolar diffusion heating rate. We are grateful to J. Chluba for helping us implement these updates.

the key to measure this effect. In this paper, we shall use the Planck 2013 temperature data [13, 14] (including the lensing data [15]) and the Planck 13 polarization likelihood [14] derived from the WMAP 9-year polarization data [16, 17] to constrain B_0 for some representative values of n_B . In particular, the lensing data play an important role in isolating the optical depth in the temperature data.

The rest of the paper is organized as follows. In section 2, we calculate the CMB temperature and polarization power spectra with a modified thermal and reionization history due to the dissipation of the magnetic field in the post decoupling era. In section 3, we obtain constraints on the magnetic field strength for some representative values of n_B . We conclude in section 4.

2 CMB anisotropies with dissipation of magnetic fields in the post-decoupling era

Dissipation of magnetic fields in the post decoupling era takes place by two processes; namely, ambipolar diffusion and decaying MHD turbulence [10]. These processes affect the evolution of the electron temperature, T_e , as

$$\dot{T}_e = -2\frac{\dot{a}}{a}T_e + \frac{x_e}{1+x_e}\frac{8\rho_\gamma\sigma_T}{3m_e c}(T_\gamma - T_e) + \frac{x_e\Gamma}{1.5k_B n_e}, \quad (2.1)$$

where the dissipation rate, $\Gamma = \Gamma_{\text{in}} + \Gamma_{\text{decay}}$, includes the contribution from ambipolar diffusion, Γ_{in} , and decaying MHD turbulence, Γ_{decay} . The other variables are: a the scale factor, T_γ the photon temperature, σ_T the Thomson scattering cross section, x_e the ionization fraction, n_e the electron number density, ρ_γ the photon energy density, m_e the electron rest mass, c the speed of light, and k_B the Boltzmann constant.

Ambipolar diffusion is due to different velocities of the neutral and the ionized matter components in the presence of a magnetic field. As this velocity difference is caused by the action of the Lorentz force on the ionized component, the dissipation rate of ambipolar diffusion is determined by the Lorentz term as [10]

$$\Gamma_{\text{in}} = \frac{\rho_n}{16\pi^2\gamma\rho_b^2\rho_i} |(\vec{\nabla} \times \vec{B}) \times \vec{B}|^2, \quad (2.2)$$

where ρ_n , ρ_i , and ρ_b are the energy densities of neutral hydrogen, ionized hydrogen, and the total baryons, respectively, and γ is the coupling between the ionized and neutral component given by $\gamma \simeq \langle\sigma v\rangle_{H^+,H}/(2m_H)$ with $\langle\sigma v\rangle_{H^+,H} = 0.649 T^{0.375} \times 10^{-9} \text{ cm}^3 \text{ s}^{-1}$ [18]. Equation (2.2) is evaluated for the average Lorentz force using the two point function of the magnetic field (cf., eq. (1.2)). The final expression depends on the magnetic field strength as well as on its spectral index, and can be found in [11].

Dissipation of the magnetic field due to decaying MHD turbulence rests on the fact that turbulence is no longer suppressed in the plasma after the decoupling epoch. On scales below the magnetic Jeans scale, the magnetic energy on large scales is transferred to small scales and dissipates. The dissipation rate of this highly non linear process is estimated by numerical simulations of MHD turbulence in flat space using the fact that there exists an appropriate rescaling of variables in flat space to match those in an expanding, flat Friedmann-Robertson-Walker background [19–24]. In the matter-dominated era, the estimated dissipation rate of

a non-helical magnetic field is given by [10]

$$\Gamma_{\text{decay}} = \frac{B_0^2}{8\pi} \frac{3m}{2} \frac{\left[\ln \left(1 + \frac{t_d}{t_i} \right) \right]^m}{\left[\ln \left(1 + \frac{t_d}{t_i} \right) + \ln \left[\left(\frac{1+z_i}{1+z} \right)^{\frac{3}{2}} \right] \right]^{m+1}} H(t) (1+z)^4, \quad (2.3)$$

where B_0 is the present-day field value assuming a flux freezing; m is related to the magnetic spectral index as $m = \frac{2(n_B+3)}{n_B+5}$; t_d is the physical decay time scale for turbulence given by $t_d/t_i = (k_J/k_d)^{\frac{(n_B+5)}{2}} \simeq 14.8 (B_0/1 \text{ nG})^{-1} (k_d/1 \text{ Mpc}^{-1})^{-1}$ with the magnetic Jeans wavenumber of $k_J \simeq 14.8 \frac{2}{n_B+5} (B_0/1 \text{ nG})^{-\frac{2}{n_B+5}} (k_d/1 \text{ Mpc}^{-1})^{\frac{n_B+3}{n_B+5}} \text{ Mpc}^{-1}$ [10]; and $z_i < z_{\text{dec}}$ and $t_i > t_{\text{dec}}$ are the redshift and time at which dissipation of the magnetic field due to decaying MHD turbulence becomes important.

Ref. [10] calculated the evolution of the matter temperature, T_e , and the ionization fraction, x_e , with the effect of damping of magnetic fields in the post decoupling era. In ref. [11], we revisited these calculations using a modified version of **Recfast++** [25–31]. We found that ambipolar diffusion contributes at $z \lesssim 100$, and the effect decreases as n_B decreases. The amplitude is proportional to B_0^4 . On the other hand, the effect of decaying MHD turbulence increases as n_B decreases, is proportional to B_0^2 , and dominates over ambipolar diffusion up to intermediate redshifts.

In figure 1 we show the evolution of T_e , x_e , the visibility function of CMB (g), and the optical depth to scattering of CMB (τ), as a function of redshift. For each choice of parameters, we show the case including the standard implementation of instantaneous reionization (denoted as “s r”) and not including it (denoted as “no s r”). We use the **CLASS** code [32–35] to compute these quantities. The standard implementation of **CLASS** is the same as in the **CAMB** code [36, 37], which uses a tanh fitting formula for the ionization fraction centered at the reionization redshift. The case not including the standard reionization is shown only for comparison. Dissipation of the decaying turbulence heats the IGM since shortly after the decoupling epoch, delaying recombination of hydrogen atoms in the IGM. At low redshifts, $z \lesssim 20$, the temperature of the completely reionized universe falls as z decreases because ambipolar diffusion cannot act on ionized plasma. In a complete treatment of the late time thermal and ionization history one should also include contributions from stellar feedback which ionizes and can efficiently heat the IGM up to temperatures of 10^4 K at $z \lesssim 10$. Since our main conclusions are not based on the temperature but on the ionization fraction, the error in the temperature evolution at $z \lesssim 20$ has no consequences. Decay of MHD turbulence increases the total optical depth to scattering of CMB shortly after the decoupling epoch, and this changes the power spectra of the temperature and polarization anisotropies, as discussed below.

We use the **CLASS** code with its standard implementation of instantaneous reionization at late times to calculate the power spectra, and show the effects of dissipation of fields in figure 2 for a magnetic field with $B_0 = 3 \text{ nG}$ and spectral indices of $n_B = -2.9, -2.5$, and -1.5 . It is well known that the optical depth to scattering of CMB suppresses the temperature and polarization power spectra by $e^{-2\tau_{\text{tot}}}$ at multipoles higher than that corresponding to the horizon size at the epoch of the scattering. In addition to the suppression due to the standard late-time reionization, the optical depth due to dissipation of fields, $\Delta\tau$, creates an additional suppression of the power spectra by $e^{-2\Delta\tau}$ (see figure 2). Also, as the peak of the visibility function of CMB shifts slightly toward a lower redshift than the standard decoupling

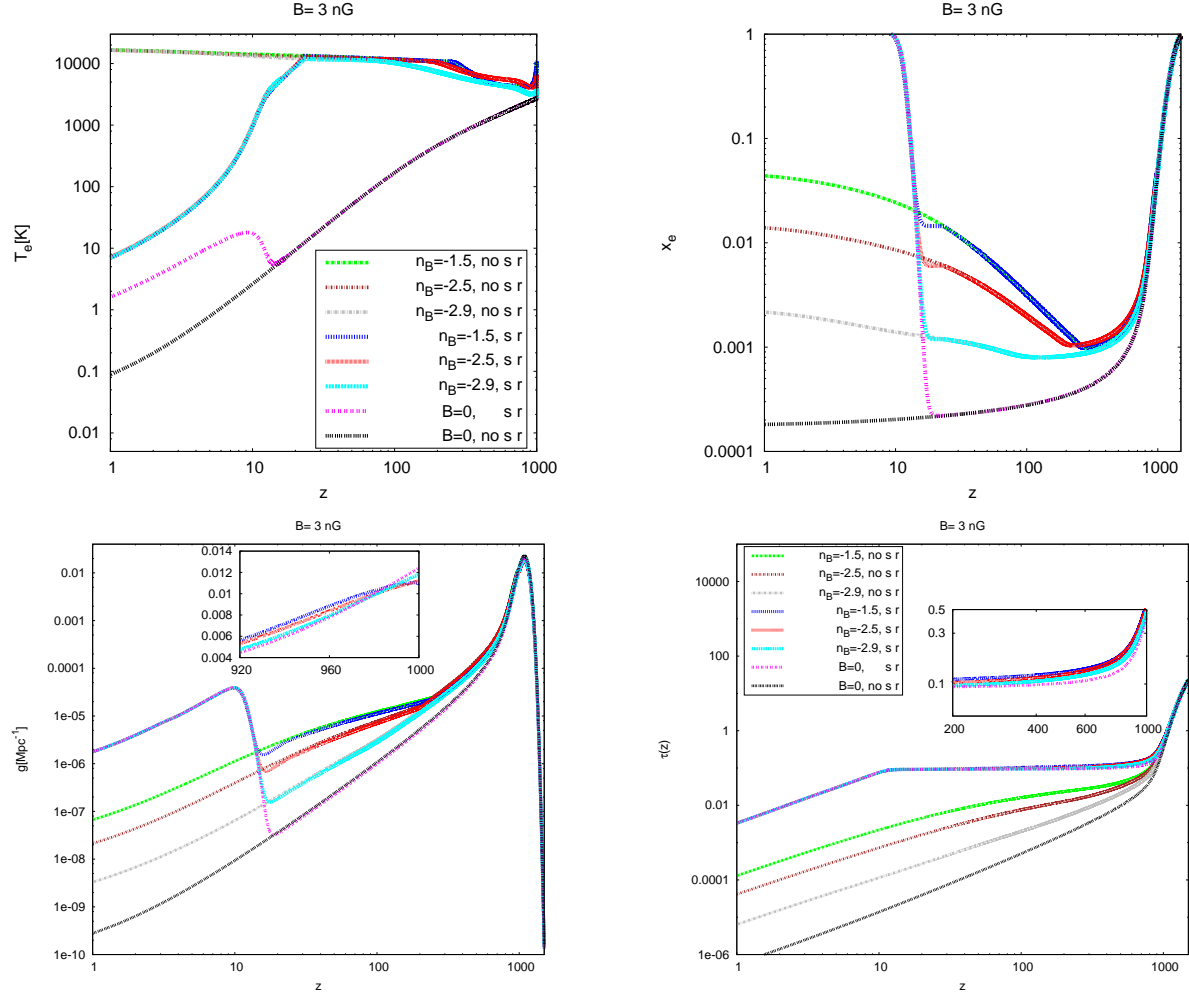


Figure 1: Evolution of the matter temperature (*top left*), the ionization fraction (*top right*), the visibility function of CMB (*bottom left*), and the total optical depth to scattering of CMB (*bottom right*), with and without dissipation of magnetic fields, and with and without the standard late-time reionization (indicated by “s r” in the legend) of the universe with $\tau_{reio} = 0.0925$. For better clarity the legend has been included only in two of the figures, though it applies to all four figures. To see the effect of dissipation of fields in the standard late-time reionization model, compare the blue, red, cyan and pink lines. The cosmological parameters are the best fit values of Planck 2013 data plus the low- ℓ polarization data of WMAP 9 [3]. The field strength is $B_0 = 3$ nG with spectral indices of $n_B = -1.5$, -2.5 , and -2.9 . At $z \gtrsim 20$, dissipation is dominated by the decaying MHD turbulence. The inset in the bottom-right panel shows an increase in the total optical depth due to decaying MHD turbulence at $z > 200$.

redshift, the angular diameter distance to the decoupling epoch is slightly reduced, shifting the locations of the acoustic peaks of the temperature and polarization power spectra to lower multipoles. This effect is more pronounced for polarization, and is clearly visible in the top right panel of figure 2.

Not only does an additional optical depth suppress the power spectra at multipoles

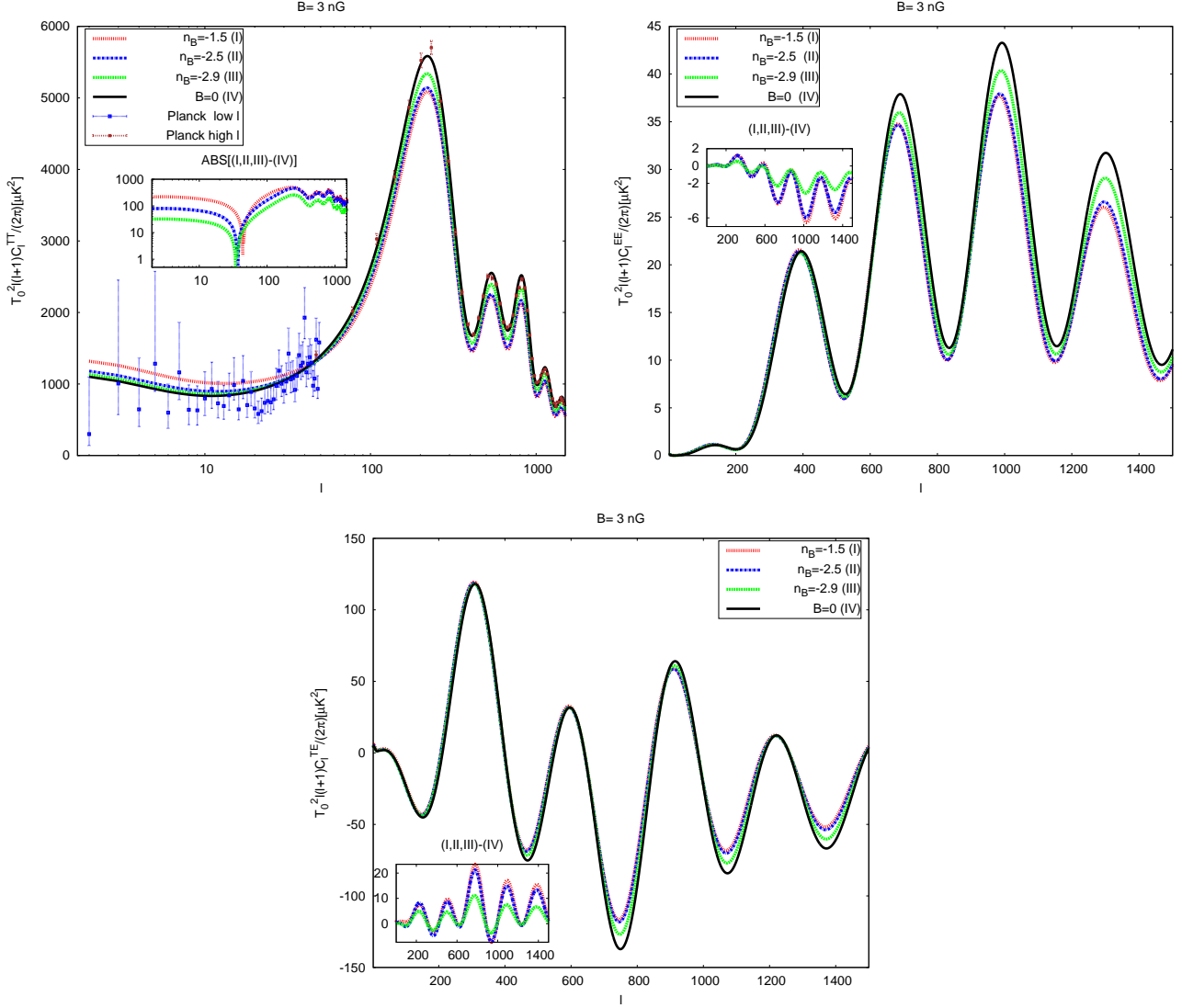


Figure 2: Temperature and polarization power spectra of CMB, with and without dissipation of magnetic fields, assuming standard late-time reionization of the universe with $\tau_{reio} = 0.0925$. The magnetic field parameters are $B_0 = 3$ nG for three different values of its spectral index n_B . The insets show the difference between each choice of spectral index and the case without the magnetic field. The additional optical depth to scattering of CMB due to dissipation of the fields suppresses the power spectra at high multipoles, while regenerating the polarization power spectra in $100 \lesssim \ell \lesssim 400$. Also, the shift of the visibility function to lower redshifts shifts the locations of the acoustic peaks of the power spectra to lower multipoles. The cosmological parameters are the best fit values of Planck 2013 data plus the Planck 13 likelihood of the low- ℓ polarization data of WMAP 9 [3]. We also show the Planck 2013 temperature data [13].

higher than that corresponding to the horizon size at the epoch of the scattering, but also creates an additional polarization *at* multipoles corresponding to the horizon size at the epoch of the scattering. The amplitudes of the first and second peaks in the *E*-mode polarization

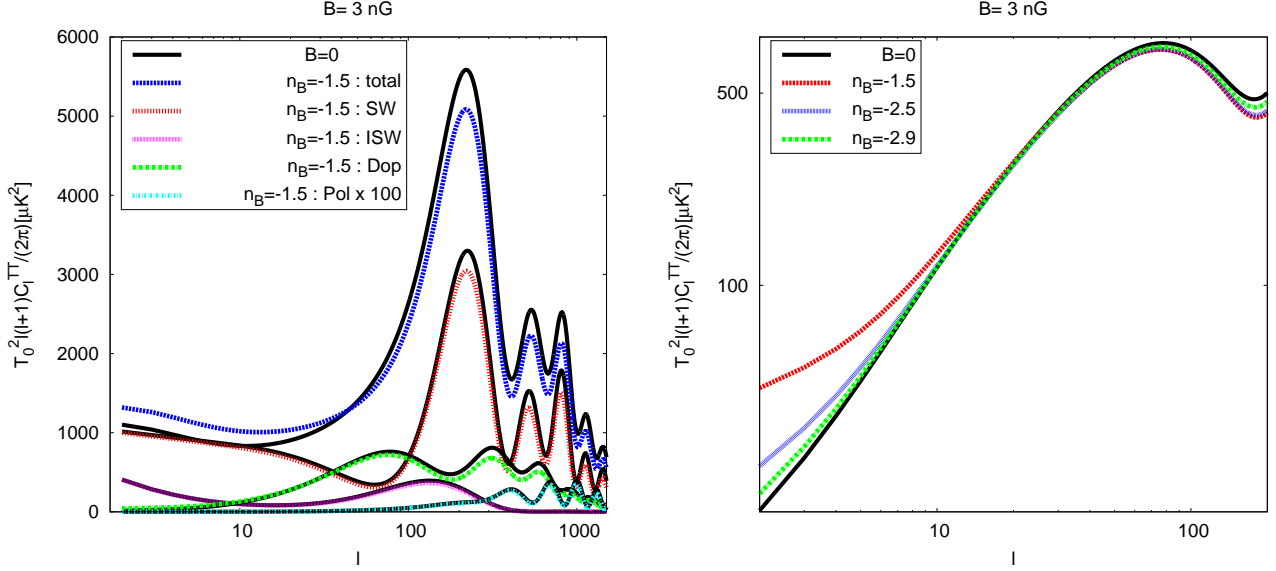


Figure 3: Temperature power spectra of CMB, with and without dissipation of magnetic fields, assuming the standard late-time reionization of the universe with $\tau_{reio} = 0.0925$. (*Left*) Contributions from the Sachs-Wolfe term (SW), the total integrated Sachs-Wolfe effect (ISW) including early and late time contributions, the Doppler term (Dop) and the polarization term (Pol). The black lines show the cases with no field, whereas the other lines show $B_0 = 3$ nG and $n_B = -1.5$. (*Right*) The Doppler term for $B = 3$ nG and $n_B = -1.5, -2.5$, and -2.9 .

power spectrum at $\ell \approx 100$ and 400 are enhanced due to regeneration of polarization by additional scattering of CMB between the decoupling and the reionization epochs. This can be seen in the top right panel of figure 2. While the polarization power spectrum at higher multipoles is significantly influenced by the change in the optical depth, that at lower multipoles is not. The “reionization bump” in the polarization power spectrum at $\ell \lesssim 10$ is not affected by dissipation of the fields, as ionization at $z \lesssim 20$ is totally dominated by that of the late-time reionization. Similar features are observed in the temperature-polarization cross power spectrum (cf. lower panel of figure 2). This phenomenology is similar to the effect of heating due to annihilation of dark matter particles [3, 38–40].

The top left panel of figure 2 shows that the low- ℓ temperature power spectrum increases with increasing magnetic spectral index. We find that this is due to an enhanced Doppler term (in Newtonian gauge). For our choice of parameters this is most noticeable for the largest spectral index, $n_B = -1.5$. In the left panel of figure 3, we show the contributions from the Sachs-Wolfe term, the integrated Sachs-Wolfe term, the Doppler term, and the polarization term to the total angular power spectrum. The right panel shows only the Doppler term, which increases as n_B increases at $\ell \lesssim 10$. This explains what we find in the top left panel of figure 2.

3 Parameter estimation

To estimate the magnetic field parameters along with the cosmological parameters, we use Markov chains Monte Carlo as implemented in `montepython` [41]. Specifically, we fix the magnetic spectral index, n_B , and vary the field strength, B_0 , along with the six standard

Λ CDM parameters, i.e., the Hubble constant, $H_0 = 100 h$ km/s/Mpc; the physical baryon density, $\omega_b \equiv \Omega_b h^2$; the physical cold dark matter density, $\omega_{cdm} \equiv \Omega_{cdm} h^2$; the amplitude of the scalar power spectrum at $k = 0.05$ Mpc $^{-1}$, A_s ; the tilt of the power spectrum, n_s ; and the optical depth from the late-time reionization, τ_{reio} .

We use the Planck 2013 temperature data [13, 14] (including the lensing data [15]) and the likelihood of the WMAP 9-year polarization data [16, 17] derived by the Planck collaboration [14]. The lensing data are essential for breaking degeneracy between A_s and B_0 . This degeneracy arises because the optical depth constraint from the temperature data is degenerate with A_s . (The temperature data effectively measure $A_s e^{-2\tau_{tot}}$.) In our study the key element is that the magnetic field dissipation significantly changes the optical depth close to decoupling and so changes the total optical depth to decoupling but does not change the optical depth to reionization. The former is determined by the temperature anisotropy data and the latter by the polarization data. The combination of the two data sets together with the lensing data allows to constrain the magnetic field parameters.

We summarize the constraints on B_0 and the cosmological parameters in table 1, and show the marginalized posterior distributions of B_0 in figure 4. We chose $n_B = -2.9$, -2.5 , and -1.5 as representative cases. We find no evidence for dissipation of the magnetic fields in the data. The 95% CL upper bounds on the field strength are $B_0 < 0.63$, 0.39 , and 0.18 nG for $n_B = -2.9$, -2.5 , and -1.5 , respectively.²

These limits are significantly stronger than those from the magnetic scalar- and vector-mode contributions to the angular power spectra of the CMB. For example, the Planck collaboration used the Planck 2013 temperature data, the WMAP 9-year polarization data, and the high- ℓ temperature data of ACT and SPT to find $B_{1\text{Mpc}} < 3.4$ nG (95% CL) for a smoothing scale of 1 Mpc from the magnetic scalar and vector modes, while ignoring the effects on the ionization history of the universe. Our limits on B_0 , which is smoothed over the magnetic damping scale at decoupling, become stronger if we scale them to a Mpc scale, as changing the smoothing scale, λ_s , to a different smoothing scale, λ_* , leads to a rescaling of the magnetic field amplitude by a factor of $(\lambda_s/\lambda_*)^{\frac{n_B+3}{2}}$.

The only limit in the literature that is stronger than ours is $B_0 < 0.01$ nG for a smoothing scale of 0.1 kpc [42], which was derived from the change in the ionization history *before* the decoupling epoch, due to the effect of clumping in the baryon density perturbations induced by a primordial magnetic field. Rescaling our limits to 0.1 kpc makes their limit much stronger than ours.

In figure 5 the two-dimensional marginalized posterior probability density distributions (B_0 versus the cosmological parameters) are shown, for $n_B = -2.9$, $n_B = -2.5$, and $n_B = -1.5$. Most of the cosmological parameters are determined independently of B_0 ; however, the scalar spectral tilt, n_s , is weakly correlated with B_0 because B_0 suppresses the power spectrum at high multipoles by $e^{-2\Delta\tau}$, which can be partly compensated by increasing n_s .

4 Conclusions

Dissipation of the magnetic fields in the post-decoupling era heats the IGM and delays recombination of hydrogen atoms. This effect can be detected as the extra optical depth to scattering of CMB photons. A qualitatively new effect is that it affects only the total optical depth to decoupling, which is determined by the temperature data together with the

²The corresponding smoothing scales are much smaller than 1 Mpc. The largest one is of order 13 kpc for $B_0 = 0.63$ nG, and 4 kpc for $B_0 = 0.18$ nG (cf. equation (1.1)).

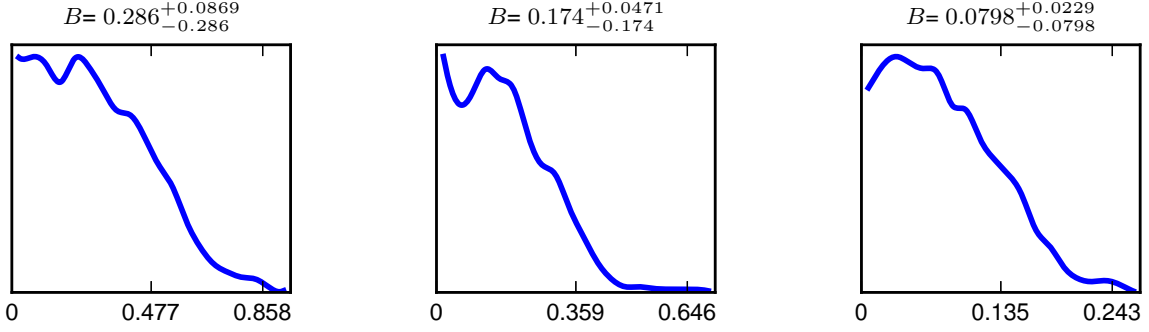


Figure 4: Marginalized posterior distributions of the magnetic field strength, B_0 (in units of nG), for the magnetic spectral index of $n_B = -2.9$ (left), $n_B = -2.5$ (middle) and $n_B = -1.5$ (right).

	$n_B = -2.9$		$n_B = -2.5$		$n_B = -1.5$	
	best-fit	68% limits	best-fit	68% limits	best-fit	68% limits
B_0	0.2176	$0.286^{+0.087}_{-0.29}$	0.154	$0.1735^{+0.047}_{-0.17}$	0.06024	$0.07979^{+0.023}_{-0.08}$
$100 \omega_b$	2.208	$2.214^{+0.027}_{-0.029}$	2.21	$2.215^{+0.027}_{-0.029}$	2.229	$2.214^{+0.028}_{-0.028}$
ω_{cdm}	0.12	$0.1188^{+0.0022}_{-0.0022}$	0.119	$0.1188^{+0.0022}_{-0.0022}$	0.1183	$0.1188^{+0.0022}_{-0.0022}$
H_0	67.22	$67.78^{+1}_{-1.1}$	67.66	$67.78^{+1}_{-1.1}$	68.14	67.74^{+1}_{-1}
$10^9 A_s$	2.172	$2.194^{+0.05}_{-0.053}$	2.225	$2.196^{+0.048}_{-0.056}$	2.188	$2.199^{+0.048}_{-0.056}$
n_s	0.9604	$0.9628^{+0.007}_{-0.0069}$	0.9663	$0.9626^{+0.0067}_{-0.007}$	0.9635	$0.9639^{+0.0074}_{-0.0075}$
τ_{reio}	0.08346	$0.08966^{+0.012}_{-0.014}$	0.09624	$0.09001^{+0.012}_{-0.014}$	0.08873	$0.08969^{+0.012}_{-0.014}$
$-\ln \mathcal{L}_{\min}$	4906.72		4906.63		4906.72	
χ^2_{\min}	9813		9813		9813	

Table 1: Best-fit values and 68% confidence limits on the present-day magnetic field strength, B_0 (in units of nG), smoothed over $k_{d,dec}$ given in equation (1.1), and the standard Λ CDM cosmological parameters.

lensing data, but not the optical depth to reionization inferred from the low- ℓ polarization data ($\ell \lesssim 10$). Using the 2013 Planck data including the CMB lensing data, together with the likelihood of the low- ℓ polarization data from WMAP as derived by the Planck collaboration, we find no evidence for the effect of dissipation of (non-helical) magnetic fields in the CMB data. The 95% CL upper bounds are $B_0 < 0.63, 0.39$, and 0.18 nG for $n_B = -2.9, -2.5$, and -1.5 , respectively. These limits are stronger than the previous limits that did not use the effect of fields on ionization history of the universe.

Inverse Compton scattering of CMB photons by hot electrons in the IGM heated by dissipating magnetic fields in the post decoupling era leads to a y -type spectral distortion [43]. For negative magnetic spectral indices, the Compton y parameter is well approximated by (see footnote 1 for the update from ref. [11])

$$y(n_B, B_0) = 1.2194 \times 10^{-5} \left(\frac{B_0}{\text{nG}} \right)^{1.7263} (-n_B)^{0.3602} - 1.2155 \times 10^{-5} \left(\frac{B_0}{\text{nG}} \right)^{1.7260} (-n_B)^{0.3619} e^{9.3978 \times 10^{-9} (-n_B)^{10.9842}}. \quad (4.1)$$

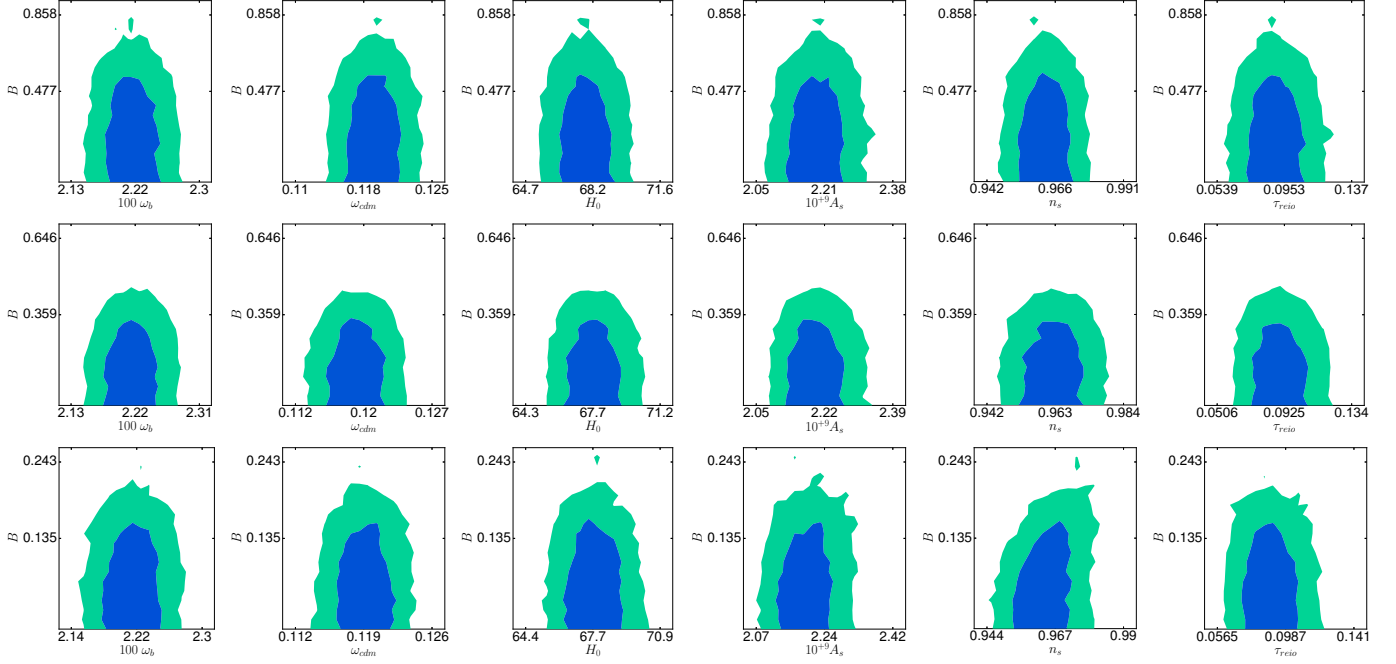


Figure 5: 68% and 95% confidence regions of the field strength, B_0 (in units of nG), versus the cosmological parameters of the Λ CDM model. The magnetic spectral indices are $n_B = -2.9$ (*upper panel*), $n_B = -2.5$ (*middle panel*), and $n_B = -1.5$ (*lower panel*).

For the upper limits on the magnetic field amplitudes derived in this paper, the resulting y -type distortions are $y < 10^{-9}$, 4×10^{-9} , and 10^{-9} for $n_B = -2.9$, -2.5 , and -1.5 , respectively. These limits are well below the contribution from the thermal Sunyaev-Zel’dovich effect in galaxy clusters and groups, $y \approx 10^{-6}$ [44], and thus are negligible.

We expect that this new method would yield much improved limits, once the full Planck data sets including high- ℓ polarization are used, as they provide significantly better measurement of the CMB lensing (which fixes A_s thus breaking degeneracy between A_s and $e^{-2\Delta\tau}$), and potentially measure the extra polarization at $100 \lesssim \ell \lesssim 400$ generated by dissipation of decaying MHD turbulence.

5 Acknowledgements

We would like to thank J. Chluba for very useful discussions. KEK would like to thank the Max-Planck-Institute for Astrophysics and the Perimeter Institute for Theoretical Physics for hospitality where part of this work was done. This research was supported in part by Perimeter Institute for Theoretical Physics. Research at Perimeter Institute is supported by the Government of Canada through Industry Canada and by the Province of Ontario through the Ministry of Economic Development & Innovation. KEK acknowledges financial support by Spanish Science Ministry grants FIS2012-30926 and CSD2007-00042. We acknowledge the use of the Legacy Archive for Microwave Background Data Analysis (LAMBDA). Support for LAMBDA is provided by the NASA Office of Space Science.

References

- [1] K. Jedamzik, V. Katalinic, and A. V. Olinto, *Damping of cosmic magnetic fields*, *Phys.Rev.* **D57** (1998) 3264–3284, [[astro-ph/9606080](#)].
- [2] K. Subramanian and J. D. Barrow, *Magnetohydrodynamics in the early universe and the damping of nonlinear Alfvén waves*, *Phys.Rev.* **D58** (1998) 083502, [[astro-ph/9712083](#)].
- [3] **Planck Collaboration** Collaboration, P. Ade et al., *Planck 2013 results. XVI. Cosmological parameters*, *Astron.Astrophys.* **571** (2014) A16, [[arXiv:1303.5076](#)].
- [4] D. Yamazaki, K. Ichiki, T. Kajino, and G. Mathews, *Constraints on the evolution of the primordial magnetic field from the small scale cmb angular anisotropy*, *Astrophys.J.* **646** (2006) 719–729, [[astro-ph/0602224](#)].
- [5] T. Kahniashvili and B. Ratra, *Effects of Cosmological Magnetic Helicity on the Cosmic Microwave Background*, *Phys.Rev.* **D71** (2005) 103006, [[astro-ph/0503709](#)].
- [6] D. Paoletti, F. Finelli, and F. Paci, *The full contribution of a stochastic background of magnetic fields to CMB anisotropies*, *Mon.Not.Roy.Astron.Soc.* **396** (2009) 523–534, [[arXiv:0811.0230](#)].
- [7] J. R. Shaw and A. Lewis, *Massive Neutrinos and Magnetic Fields in the Early Universe*, *Phys.Rev.* **D81** (2010) 043517, [[arXiv:0911.2714](#)].
- [8] K. E. Kunze, *Effects of helical magnetic fields on the cosmic microwave background*, *Phys.Rev.* **D85** (2012) 083004, [[arXiv:1112.4797](#)].
- [9] **Planck Collaboration** Collaboration, P. Ade et al., *Planck 2015 results. XIX. Constraints on primordial magnetic fields*, [arXiv:1502.0159](#).
- [10] S. K. Sethi and K. Subramanian, *Primordial magnetic fields in the post-recombination era and early reionization*, *Mon.Not.Roy.Astron.Soc.* **356** (2005) 778–788, [[astro-ph/0405413](#)].
- [11] K. E. Kunze and E. Komatsu, *Constraining primordial magnetic fields with distortions of the black-body spectrum of the cosmic microwave background: pre- and post-decoupling contributions*, *JCAP* **01** (2014) 009, [[arXiv:1309.7994](#)].
- [12] J. Chluba, D. Paoletti, F. Finelli, and J.-A. Rubino-Martin, *Effect of primordial magnetic fields on the ionization history*, [arXiv:1503.0482](#).
- [13] **Planck Collaboration** Collaboration, P. Ade et al., *Planck 2013 results. I. Overview of products and scientific results*, *Astron.Astrophys.* **571** (2014) A1, [[arXiv:1303.5062](#)].
- [14] **Planck Collaboration** Collaboration, P. Ade et al., *Planck 2013 results. XV. CMB power spectra and likelihood*, *Astron.Astrophys.* **571** (2014) A15, [[arXiv:1303.5075](#)].
- [15] **Planck Collaboration** Collaboration, P. Ade et al., *Planck 2013 results. XVII. Gravitational lensing by large-scale structure*, *Astron.Astrophys.* **571** (2014) A17, [[arXiv:1303.5077](#)].
- [16] **WMAP Collaboration**, C. Bennett et al., *Nine-Year Wilkinson Microwave Anisotropy Probe (WMAP) Observations: Final Maps and Results*, *Astrophys.J.Suppl.* **208** (2013) 20, [[arXiv:1212.5225](#)].
- [17] **WMAP Collaboration**, G. Hinshaw et al., *Nine-Year Wilkinson Microwave Anisotropy Probe (WMAP) Observations: Cosmological Parameter Results*, *Astrophys.J.Suppl.* **208** (2013) 19, [[arXiv:1212.5226](#)].
- [18] D. R. Schleicher, R. Banerjee, and R. S. Klessen, *Reionization - A probe for the stellar population and the physics of the early universe*, *Phys.Rev.* **D78** (2008) 083005, [[arXiv:0807.3802](#)].
- [19] M. Christensson, M. Hindmarsh, and A. Brandenburg, *Inverse cascade in decaying 3-D magnetohydrodynamic turbulence*, *Phys.Rev.* **E64** (2001) 056405, [[astro-ph/0011321](#)].

- [20] A. Brandenburg, K. Enqvist, and P. Olesen, *Large scale magnetic fields from hydromagnetic turbulence in the very early universe*, *Phys.Rev.* **D54** (1996) 1291–1300, [[astro-ph/9602031](#)].
- [21] R. Banerjee and K. Jedamzik, *Are cluster magnetic fields primordial?*, *Phys.Rev.Lett.* **91** (2003) 251301, [[astro-ph/0306211](#)].
- [22] W.-C. Muller and D. Biskamp, *Scaling Properties of Three-Dimensional Magnetohydrodynamic Turbulence*, *Phys.Rev.Lett.* **84** (2000) 475–478.
- [23] P. Olesen, *On inverse cascades in astrophysics*, *Phys.Lett.* **B398** (1997) 321–325, [[astro-ph/9610154](#)].
- [24] T. Shiromizu, *Inverse cascade of primordial magnetic field in MHD turbulence*, *Phys.Lett.* **B443** (1998) 127–130, [[astro-ph/9810339](#)].
- [25] S. Seager, D. D. Sasselov, and D. Scott, *A new calculation of the recombination epoch*, *Astrophys.J.* **523** (1999) L1–L5, [[astro-ph/9909275](#)].
- [26] S. Seager, D. D. Sasselov, and D. Scott, *How exactly did the universe become neutral?*, *Astrophys.J.Suppl.* **128** (2000) 407–430, [[astro-ph/9912182](#)].
- [27] W. Y. Wong, A. Moss, and D. Scott, *How well do we understand cosmological recombination?*, *Mon.Not.Roy.Astron.Soc.* (2007) [[arXiv:0711.1357](#)].
- [28] J. Chluba and R. M. Thomas, *Towards a complete treatment of the cosmological recombination problem*, *Mon.Not.Roy.Astron.Soc.* **412** (2011) 748–764, [[arXiv:1010.3631](#)].
- [29] J. A. Rubiño-Martín, J. Chluba, W. A. Fendt, and B. D. Wandelt, *Estimating the impact of recombination uncertainties on the cosmological parameter constraints from cosmic microwave background experiments*, *Mon.Not.Roy.Astron.Soc.* **403** (2010) 439–452, [[arXiv:0910.4383](#)].
- [30] J. Chluba, *Could the cosmological recombination spectrum help us understand annihilating dark matter?*, *Mon.Not.Roy.Astron.Soc.* **402** (2010) 1195–1207, [[arXiv:0910.3663](#)].
- [31] J. Chluba, G. M. Vasil, and L. J. Dursi, *Recombinations to the Rydberg states of hydrogen and their effect during the cosmological recombination epoch*, *Mon.Not.Roy.Astron.Soc.* **407** (2010) 599–612, [[arXiv:1003.4928](#)].
- [32] J. Lesgourgues, *The Cosmic Linear Anisotropy Solving System (CLASS) I: Overview*, [[arXiv:1104.2932](#)].
- [33] D. Blas, J. Lesgourgues, and T. Tram, *The Cosmic Linear Anisotropy Solving System (CLASS) II: Approximation schemes*, *JCAP* **1107** (2011) 034, [[arXiv:1104.2933](#)].
- [34] J. Lesgourgues, *The Cosmic Linear Anisotropy Solving System (CLASS) III: Comparision with CAMB for LambdaCDM*, [[arXiv:1104.2934](#)].
- [35] J. Lesgourgues and T. Tram, *The Cosmic Linear Anisotropy Solving System (CLASS) IV: efficient implementation of non-cold relics*, *JCAP* **1109** (2011) 032, [[arXiv:1104.2935](#)].
- [36] A. Lewis, A. Challinor, and A. Lasenby, *Efficient computation of CMB anisotropies in closed FRW models*, *Astrophys.J.* **538** (2000) 473–476, [[astro-ph/9911177](#)].
- [37] A. Lewis, *Cosmological parameters from WMAP 5-year temperature maps*, *Phys.Rev.* **D78** (2008) 023002, [[arXiv:0804.3865](#)].
- [38] S. Galli, F. Iocco, G. Bertone, and A. Melchiorri, *CMB constraints on Dark Matter models with large annihilation cross-section*, *Phys.Rev.* **D80** (2009) 023505, [[arXiv:0905.0003](#)].
- [39] D. P. Finkbeiner, S. Galli, T. Lin, and T. R. Slatyer, *Searching for Dark Matter in the CMB: A Compact Parameterization of Energy Injection from New Physics*, *Phys.Rev.* **D85** (2012) 043522, [[arXiv:1109.6322](#)].
- [40] G. Giesen, J. Lesgourgues, B. Audren, and Y. Ali-Haïmoud, *CMB photons shedding light on dark matter*, *JCAP* **1212** (2012) 008, [[arXiv:1209.0247](#)].

- [41] B. Audren, J. Lesgourgues, K. Benabed, and S. Prunet, *Conservative Constraints on Early Cosmology: an illustration of the Monte Python cosmological parameter inference code*, *JCAP* **1302** (2013) 001, [[arXiv:1210.7183](#)].
- [42] K. Jedamzik and T. Abel, *Small-scale primordial magnetic fields and anisotropies in the cosmic microwave background radiation*, *JCAP* **1310** (2013) 050.
- [43] K. Jedamzik, V. Katalinic, and A. V. Olinto, *A Limit on primordial small scale magnetic fields from CMB distortions*, *Phys.Rev.Lett.* **85** (2000) 700–703, [[astro-ph/9911100](#)].
- [44] A. Refregier, E. Komatsu, D. N. Spergel, and U.-L. Pen, *Power spectrum of the Sunyaev-Zel’dovich effect*, *Phys.Rev.* **D61** (2000) 123001, [[astro-ph/9912180](#)].